WATER PERMEABILITY MEASUREMENTS ON HYDRATE-SATURATED SANDSTONE CORES WITH IMMOBILE GAS

Stian Almenningen and Geir Ersland
Department of Physics and Technology, University of Bergen

This paper was prepared for presentation at the International Symposium of the Society of Core Analysts held in Vienna, Austria, 27 August – 1 September 2017.

ABSTRACT

Water permeability values for hydrate-bearing sandstone cores are presented and compared with existing theoretical flow models for water through hydrate-filled sediments. Differential pressure has been measured from constant flow injection of brine into Bentheim sandstone cores presaturated with methane hydrate and the permeability is calculated based on Darcy's law. Initial water saturation prior to hydrate formation has been ranging between 0.72 and 0.95, aimed at mimicking the natural hydrate growth process from dissolved methane in water and keeping the potential final gas saturation low and immobile. The results show that the permeability is decreasing towards zero at a hydrate saturation of around 0.50 when hydrate formation has been initiated with some free gas (approximately 0.20-0.30) in the core. In this case, the growth process is believed to start at the gas/water interface that exists throughout the pore network. Hydrate formation from a completely water saturated core resulted in a hydrate saturation of only 0.19 but the corresponding permeability was nearly zero. Heterogeneous hydrate growth at the end surfaces of the core is assumed to account for this observation. Theoretical permeability models are also reviewed and compared with the findings of this study. Accurate predictions of water permeability in hydrate sediments are important to assess production of methane gas from hydrate deposits. The presented permeability values can be used to calibrate reservoir simulators and will enhance the knowledge of flow potential in hydrate reservoirs.

INTRODUCTION

Natural gas hydrates are one promising energy resource that can contribute to the world's future energy demand, acting as a gap between conventional fossil fuels (coal and oil) and completely renewable energy sources. Production of hydrates yields methane gas which has a low carbon footprint compared to coal and oil, and one proposed production method gives an additional environmental effect by allowing injected CO_2 to be stored in the formation as methane gas is harvested [1]. The energy potential is huge as even extraction of only the most promising hydrate deposits (arctic sandstones under existing infrastructure) will give 10's of TCF surplus of methane gas to the global energy market [2].

As with production of conventional gas and oil, mining of methane hydrates rely on sufficient permeability to permit flow of liberated gas and water. Gas hydrates are also of interest as a sealing mechanism related to CO_2 storage in saline aquifers [3]. In either way, knowledge of permeability alteration in response to hydrate saturation is important to assess the potential of production or sealing.

Some experimental studies have previously been published on permeability in hydrate-saturated porous media: effective gas permeability measurements [4-9], effective water permeability measurements [7, 10-12], and two-phase flow [13-15]. Noticeable differences in relative permeability to water ($k_{rw} \approx 0.1$ at $S_H = 0.45$ and residual gas [11], $k_{rw} \approx 0.02$ at $S_H = 0.09$ and residual gas [10], and $k_{rw} \approx 0.004$ at $S_H = 0.07$ and residual gas [15]), shows the importance of phase distribution on permeability and that extensive permeability measurements are needed to calibrate permeability models.

This study is a continuation of the work presented in Almenningen *et al.* [9] where effective permeability to gas was measured in sandstone containing hydrate and immobile water. A critical gas saturation of 0.34-0.38 was identified where the gas permeability dropped from mD to µD range (S_H ranging from 0.37 to 0.61). Effective permeability to water has been measured in this study for the same range of hydrate saturation and with immobile gas. The aim of this experimental work is to identify the equivalent critical saturation of water and also to provide experimental values needed to validate permeability correlations.

Review of Permeability Models

A comprehensive review of permeability models applicable to hydrate-saturated porous media is previously given by Kleinberg *et al.* [12]. This section will provide a to-the-point overview of available permeability correlations mainly built on the work provided by Kleinberg *et al.* [12]. The models are later used to evaluate the permeability values found in this experimental study.

One of the simplest way to model flow through porous media is by assuming that flow conduits consist of straight cylindrical channels with constant cross-sectional area. The Poiseuille's equation describes flow through circular tubes and the permeability of a media consisting of *n* tubes becomes:

$$k = \frac{n\pi r^4}{8A} = \frac{\Phi r^2}{8}, \quad (1)$$

where r [m] is the radius of the tubes, A [m^2] is the cross-sectional area of the media and Φ [fraction] is the porosity of the media. The reduction in permeability with hydrate saturation will then depend on how the hydrate distributes within the pores. If hydrate coats the cylindrical walls with a uniform layer the permeability reduces to:

$$k = \frac{\phi r^2 (1-S_H)^2}{8} \Rightarrow \quad k_{rw} = (1-S_H)^2, \tag{2}$$

where S_H [fraction] is the hydrate saturation and k_{rw} [fraction] is the relative permeability to water. If hydrate is located in the center of the cylindrical pores and grows radially outwards, the permeability relation becomes:

$$k = \frac{\phi r^2}{8}\left(1 - S_H^2 - \frac{(1-S_H)^2}{\log\left(\frac{1}{S_H^{0.5}}\right)}\right) \Rightarrow k_{rw} = 1 - S_H^2 + \frac{2(1-S_H)^2}{logS_H}. \tag{3}$$

These permeability correlations for grain-coating and pore-filling hydrate growth are rigorous but lack realism in their assumptions. The pore network of authentic rocks consists of tortuous channels where the actual flow path is longer than the length of the medium. Pores are also varying in size and shape, and the wetting properties of the solid grains will influence on where hydrate forms in the pore space. Kleinberg *et al.* [12] tried to derive more realistic permeability relations, starting from a Kozeny equation of permeability and introducing the relation between saturation changes and electrical properties from the work of Hearst *et al.* [16] and Spangenberg [17]. The relative permeability of water, when hydrate coats grains, becomes:

$$k_{rw} = (1-S_H)^{n+1}, \tag{4}$$

and for hydrate growing in the center of pores, the relative permeability becomes:

$$k_{rw} = \frac{(1-S_H)^{n+2}}{\left(1+S_H^{0.5}\right)^2}, \tag{5}$$

where n is the saturation exponent from Archie's relations. This exponent is not easy to obtain as it will change during hydrate growth [17], and the derivation of the equations is also neglecting the change in the cementation exponent m during hydrate growth. A generalization of Equation 2 that is widely used to compare with experimental data originates from Masuda *et al.* [18]:

$$k_{rw} = (1-S_H)^N, \tag{6}$$

where N acts as a fitting parameter. Masuda *et al.* [18] chose N = 10 and 15 to account for hydrate growth in pore throats, but a variety of values have been found by fitting the equation to experimental data: N = 3-5 [4], N = 8-9 [5], N = 7.7-9.4 [19], and N = 38 [10].

Another permeability relation that is also based on a Kozeny equation, and that is developed by modelling of a 2D pore network containing different hydrate distributions, is [20]:

$$k_{rw} = \frac{(1-S_H)^3}{(1+2S_H)^2}. \quad (7)$$

This equation takes into account the change in tortuosity and specific surface area due to hydrate formation.

The reservoir simulator TOUGH+HYDRATE v1.5 reduces the absolute permeability during hydrate growth according to the reduction in porosity and the user can then choose from many different relative permeability correlations, such as Corey's [21] and Grant's curves [22]. The absolute permeability reduction is given by:

$$\frac{k}{k_0} = \left(\frac{\phi-\phi_c}{\phi_0-\phi_c}\right)^n, \quad (8)$$

where the subscript *0* denotes reference state and Φ_c is a non-zero critical porosity where the permeability *k* is zero. The exponent *n* is reported to be in the range from 2 to 3 but can also be as large as *n* = 10 or more, depending on how hydrate grows in the pore space (Moridis and Pruess [23], and references therein).

Equations 2-7 are applicable if hydrate forms from water saturated with methane gas (one phase, two components). If a gas phase is present after hydrate formation, two-phase flow models should be applied to model the relative permeability of water and gas under the influence of solid hydrates. Equations 2-7 can nonetheless be used for water flow if the residual gas present after hydrate formation is assumed immobile. However, the measured water permeability will then be expected to be lower than predicted by Equations 2-7 because of the extra flow restriction offered by the stationary gas phase.

EXPERIMENTAL PROCEDURE

Cylindrical Bentheim sandstone cores (length ≈ 15 cm and diameter ≈ 5 cm) were used as porous medium. They have fairly constant porosity and absolute permeability of 0.22-0.24 and 0.9-1.1 D, respectively. Every core was saturated to a predefined value (ranging from 0.72 to 0.95) with brine and then mounted into the rubber sleeve inside the core holder. Salinity values of 0.1, 1.0, 2.0, 2.5, 3.0, 3.5 and 4.0 wt% NaCl were used to customize the final hydrate saturation. All pump lines and tubes were purged under vacuum before filling the pump with methane gas (>99.5%). The core was pressurized to 8.3 MPa from both ends and the overburden pressure was applied to the sleeve by pressurized oil (3 MPa above pore pressure). Hydrate formation was initiated by circulation of antifreeze through a cooling jacket that surrounds the core holder and that reduced the temperature to a constant 4°C for all tests. Hydrate growth was finalized when the consumption of methane gas stopped, and permeability measurements were performed by injecting brine (same salinity as the initial brine saturating the core) from one side of the core. Another pump containing the same brine

was connected to the other side of the core and was set to hold a constant pressure of 8.3 MPa. Differential pressure was monitored and recorded as the pressure drop stabilized across the core during constant volume rate injection. The permeability of each hydrate-saturated core was calculated by Darcy's law. Temperature sensors placed at the inlet and outlet core ends were used to monitor the temperature evolution during injection. The injected water was not pre-cooled, but low injection rates (< 0.03 mL/min) assured no temperature increase and corresponding hydrate dissociation during permeability measurements. The reader is referred to Almenningen *et al.* [9] for details of the experimental set-up.

RESULTS AND DISCUSSION

A total of nine flow experiments were conducted to investigate the water permeability of hydrate-saturated sandstone cores. High initial brine saturations varying between 0.72 and 0.95, together with salinities ranging between 0.1 and 4.0 wt% NaCl, resulted in final hydrate saturations between 0.19 and 0.60 (Table 1). The residual gas saturation after hydrate formation did not exceed 0.18 and the gas phase was considered immobile during water flow. No produced methane gas was observed in the production pump for all experiments.

The water permeability followed an increasing trend with increasing water saturation but remained low for all saturations of water (Figure 1). The maximum permeability was observed to be in the order of 100-200 µD at the highest water saturation of approximately 0.55, which corresponds to a relative permeability in the order of 0.0001. This shows the major impact of hydrates on permeability and is also reflected in the critical water saturation where permeability dropped to zero. Measurable permeability values were not obtained at water saturations lower than 0.40, while the critical water saturation for regular two phase flow (water and gas) is lower than 0.20 for Bentheim sandstone [24].

The objective to create hydrate from one phase (dissolved methane in water) by saturating the cores completely with brine was not achieved. Upon cooling of the core, no injection of gas followed as it would do during hydrate growth due to up-concentration of gas in the hydrate phase. The best attempt of creating hydrate from high initial brine saturation was accomplished during experiment 2 (S_{wi} = 0.95). However, the final hydrate saturation became only 0.19 as hydrate growth initiated at the gas/water interface in both core ends. Further growth diminished when the solid hydrate film blocked for methane transport inwards in the core into the water phase. Consequently, the resulting permeability became close to zero despite the low hydrate saturation. The possibility of additional hydrate formation from dissolved methane inside the core cannot be ruled out as the experiment was conducted without *in situ* monitoring and information about growth characteristics relied solemnly on pressure communication with the pump.

Permeability measurements have traditionally been used in conjunction with ultrasonic and electrical measurements to estimate hydrate growth habit. Either pore-filling or pore-coating growth are suggested by comparing experimental values to the predictions of Equations 3 (or 5) and 2 (or 4), respectively. Some studies indicate pore-filling hydrate growth [5, 7, 12, 15], while other point to a shift from pore-coating to pore-filling hydrate growth as the hydrate saturation reaches a certain value [4, 11]. A hybrid modelling approach has also been developed which consists of a weighted combination of Equations 4 and 5 [25]. The permeability measured in this study is not comparable to the predictions of Equations 2-5 nor 7. Only Equations 6 and 8 can match the experimental values; with $N = 14$ and $n = 7$, respectively, giving the best fit (Figure 2). The findings imply that the assumption of either pore-filling or pore-coating hydrate growth is too simplistic and that the permeability evolution is highly influenced by heterogeneous growth. Hydrate occupying pore throats close to the core ends may explain the observed low permeability in this study. Building of permeability correlations should therefore be assisted with *in situ* monitoring of hydrate distribution to account for effects originating from different preparation methods and experimental procedures.

CONCLUSIONS

Effective permeability to water was measured for nine cylindrical sandstone cores filled with methane hydrate saturations ranging between 0.19-0.60 and immobile gas. The effective permeability to water was consistently low for all combinations of saturation, decreasing from an upper level of 100-200 µD and down to zero permeability at a water saturation of approximately 0.40. For comparison, the absolute permeability of the cores was 0.9-1.1 D. The measured permeability values were order of magnitudes lower than what was predicted by existing permeability correlations with fixed parameters. Only equations containing fitting parameters could simulate the experimental results.

REFERENCES

1. Graue, A., B. Kvamme, B. Baldwin, J. Stevens, J.J. Howard, E. Aspenes, G. Ersland, J. Husebø and D. Zornes, "MRI Visualization of Spontaneous Methane Production From Hydrates in Sandstone Core Plugs When Exposed to CO2". *SPE Journal*, (2008) **13**(2): p. 146-152.
2. Boswell, R. and T.S. Collett, "The Gas Hydrates Resource Pyramid". *Fire in the Ice* (The National Energy Technology Laboratory Methane Hydrate Newsletter), (2006) **Fall**: p. 5-7.
3. Kvamme, B., A. Graue, T. Buanes, T. Kuznetsova and G. Ersland, "Storage of CO2 in natural gas hydrate reservoirs and the effect of hydrate as an extra sealing in cold aquifers". *International Journal of Greenhouse Gas Control*, (2007) **1**(2): p. 236-246.

4. Kumar, A., B. Maini, P.R. Bishnoi, M. Clarke, O. Zatsepina and S. Srinivasan, "Experimental determination of permeability in the presence of hydrates and its effect on the dissociation characteristics of gas hydrates in porous media". *Journal of Petroleum Science and Engineering*, (2010) **70**(1–2): p. 114-122.
5. Liang, H., Y. Song, Y. Chen and Y. Liu, "The Measurement of Permeability of Porous Media with Methane Hydrate". *Petroleum Science and Technology*, (2011) **29**(1): p. 79-87.
6. Chuvilin, E., S. Grebenkin and E. Tkacheva, "CHANGE OF GAS PERMEABILITY OF GAS-SATURATED SEDIMENTS DURING HYDRATE FORMATION AND FREEZING", in *Proceedings of the 8th International Conference on Gas Hydrates*, (2014), Beijing, China.
7. Kneafsey, T.J., Y. Seol, A. Gupta and L. Tomutsa, "Permeability of Laboratory-Formed Methane-Hydrate-Bearing Sand: Measurements and Observations Using X-Ray Computed Tomography". *SPE Journal*, (2011) **16**(1): p. 78-94.
8. Ersland, G., J. Husebø, A. Graue, B. Kvamme, B. Baldwin, J. Howard and J. Stevens, "Measurements of Gas Permeability and Non-Darcy Flow in Gas-Water-Hydrate Systems", in *Proceedings of the 6th International Conference on Gas Hydrates*, (2008), Vancouver, Canada.
9. Almenningen, S., H. Juliussen and G. Ersland. "Permeability measurements on hydrate-bearing sandstone cores with excess water", in *The 30th International Symposium of the Society of Core Analysts*, (2016), Snowmass, Colorado.
10. Li, B., X.S. Li, G. Li, J.L. Jia and J.C. Feng, "Measurements of Water Permeability in Unconsolidated Porous Media with Methane Hydrate Formation". *Energies*, (2013) **6**(7): p. 3622-3636.
11. Delli, M.L. and J.L.H. Grozic, "Experimental determination of permeability of porous media in the presence of gas hydrates". *Journal of Petroleum Science and Engineering*, (2014) **120**: p. 1-9.
12. Kleinberg, R.L., C. Flaum, D.D. Griffin, P.G. Brewer, G.E. Malby, E.T. Peltzer and J.P. Yesinowski, "Deep sea NMR: Methane hydrate growth habit in porous media and its relationship to hydraulic permeability, deposit accumulation, and submarine slope stability". *JOURNAL OF GEOPHYSICAL RESEARCH*, (2003) **108**(B10): p. 1-17.
13. Johnson, A., S. Patil and A. Dandekar, "Experimental investigation of gas-water relative permeability for gas-hydrate-bearing sediments from the Mount Elbert Gas Hydrate Stratigraphic Test Well, Alaska North Slope". *Marine and Petroleum Geology*, (2011) **28**(2): p. 419-426.
14. Ahn, T., J. Lee, D.G. Huh and J.M. Kang, "Experimental Study on Two-phase Flow in Artificial Hydrate-bearing Sediments". *Geosystem Engineering*, (2005) **8**(4): p. 101-104.
15. Jaiswal, N.J., A. Dandekar, S. Patil, R.B. Hunter and T.S. Collett, "Relative Permeability Measurements of Gas-water-hydrate Systems". *Natural gas hydrates - Energy resource potential and associated geologic hazards: AAPG Memoir*, (2009) **89**: p. 723-733.
16. Hearst, J.R., P.H. Nelson and F.L. Paillet, *Well Logging for Physical Properties*. (2000) New York: McGraw-Hill.

17. Spangenberg, E., "Modeling of the influence of gas hydrate content on the electrical properties of porous sediments". *Journal of Geophysical Research: Solid Earth*, (2001) **106**(B4): p. 6535-6548.
18. Masuda, Y., S. Naganawa, S. Ando and K. Sato, "Numerical calculation of gas production performance from reservoirs containing natural gas hydrates", in *Annual Technical Conference*, (1997), San Antonio, Texas.
19. Konno, Y., Y. Jin, T. Uchiumi and J. Nagao, "Multiple-pressure-tapped core holder combined with X-ray computed tomography scanning for gas–water permeability measurements of methane-hydrate-bearing sediments". *Review of Scientific Instruments*, (2013) **84**(6): p. 064501.
20. Dai, S. and Y. Seol, "Water permeability in hydrate-bearing sediments: A pore-scale study". *Geophysical Research Letters*, (2014) **41**(12): p. 4176-4184.
21. Corey, A.T., "The Interrelation Between Gas and Oil Relative Permeabilities". *Producers Monthly*, (1954) November: p. 38-41.
22. Grant, M.A., "Permeability Reduction Factors at Wairakei", paper 77-HT-52, in *AICHE-ASME Heat Transfer Conference*, (1977), Salt Lake City, Utah.
23. Moridis, G.J. and K. Pruess, "User's Manual of the Tough+ Core Code v1.5: A General-Purpose Simulator of Non-Isothermal Flow and Transport Through Porous and Fractured Media", Report LBNL-6871E, Lawrence Berkeley National Laboratory, Berkeley, California, (2014).
24. Teige, G.M.G., W.L.H. Thomas, C. Hermanrud, P.E. Øren, L. Rennan, O.B. Wilson and H.M.N. Bolås, "Relative permeability to wetting-phase water in oil reservoirs". *Journal of Geophysical Research: Solid Earth*, (2006) **111**(B12): p. 1-20.
25. Delli, M.L. and J.L.H. Grozic, "Prediction Performance of Permeability Models in Gas-Hydrate-Bearing Sands". *SPE Journal*, (2013) **18**(2).

Table 1. List of all experiments with related saturations and permeability values. Margins of error reflect equipment uncertainties.

Experiment ID	**S_{wi}** ±0.01	**Salinity** [wt% NaCl]	**S_{wf}** ±0.02	**S_H** ±0.02	**S_g** ±0.02	**K** [µD]
1	0.78	0.1	0.30	0.60	0.10	0
2	0.95	0.1	0.80	0.19	0.01	1.1 ±0.7
3	0.80	2.0	0.43	0.47	0.10	17 ±2
4	0.74	2.5	0.41	0.41	0.18	3.9 ±0.2
5	0.80	3.0	0.46	0.44	0.10	26 ±3
6	0.79	3.5	0.55	0.32	0.13	108 ±16
7	0.80	3.5	0.51	0.37	0.12	62 ±9
8	0.80	3.5	0.52	0.36	0.12	176 ±37
9	0.72	4.0	0.35	0.48	0.17	0

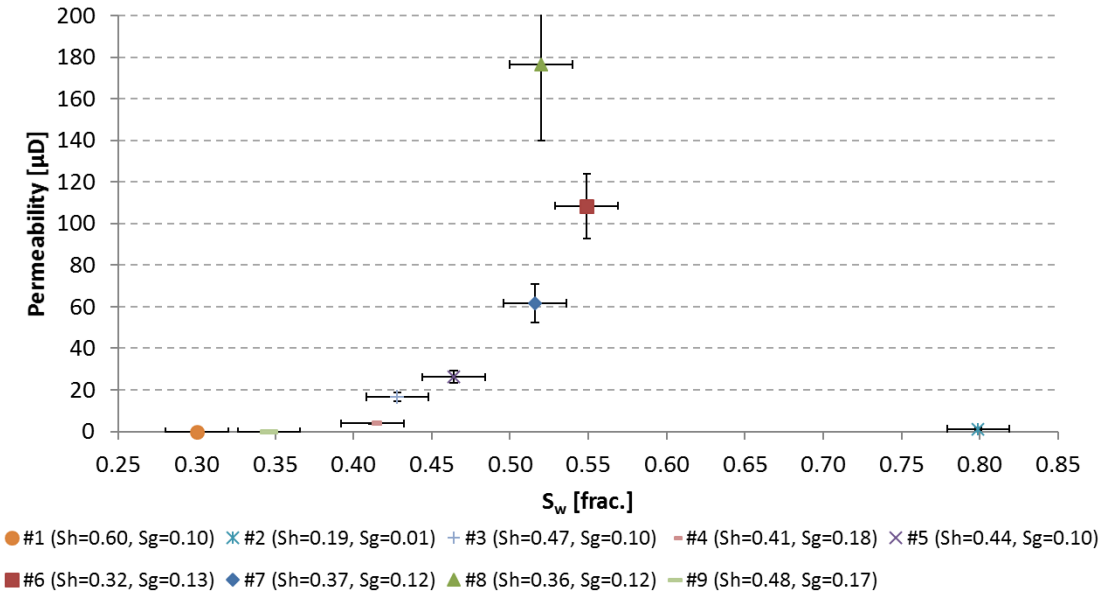

Figure 1. Water permeability after hydrate formation. Experiment 2 had close to zero permeability, despite having a high final water saturation, because of heterogeneous hydrate accumulation at the core ends. Margins of error reflect equipment uncertainties.

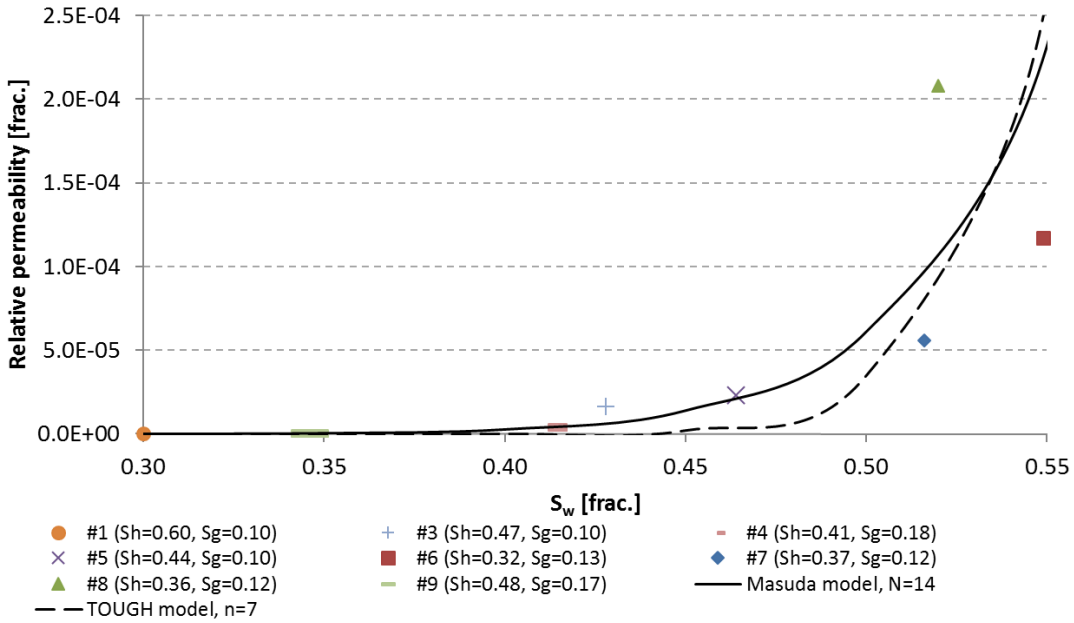

Figure 2. Comparison between experimentally obtained values of relative permeability to water and theoretical permeability values. Experiment 2 has been excluded from the graph because of heterogeneous hydrate growth. Only the models of Masuda and TOUGH+HYDRATE predicted permeability values comparable to experimental data, with a best fit achieved with $N = 14$ and $n = 7$, respectively.